

11:27:35

OCA PAD INITIATION - PROJECT HEADER INFORMATION

05/21/92

Active

Project #: E-27-661 Cost share #: Rev #: 0
Center # : 10/24-6-R7489-0A0 Center shr #: OCA file #:
Contract#: F3360192MY642 Mod #: Work type : RES
Prime # : Document : PO
Contract entity: GTRC

Subprojects ? : N CFDA:
Main project #: PE #: 622000

Project unit: TEXT ENGR Unit code: 02.010.130
Project director(s):
KUMAR S TEXT ENGR (404)853-9346

Sponsor/division names: AIR FORCE / WRIGHT-PATTERSON AFB, OH
Sponsor/division codes: 104 / 002

Award period: 920509 to 920815 (performance) 920930 (reports)

Sponsor amount	New this change	Total to date
Contract value	12,000.00	12,000.00
Funded	12,000.00	12,000.00
Cost sharing amount		0.00

Does subcontracting plan apply?: N

Title: UNDERSTANDING THE HIERARCHIAL STRUCTURE IN THE LIQUID CRYSTALLING POLYMERIC..

PROJECT ADMINISTRATION DATA

OCA contact: E. Faith Gleason 894-4820

Sponsor technical contact	Sponsor issuing office
DR. ANTHONY PALAZOTTO (513)255-3069	MS. PAM SPRAY, OPERATIONAL CONTR DIV (513)257-8272
AFIT/ENY BLDG. 640, AREA B WRIGHT-PATTERSON AFB, OH 45433-6583	HQ WPCC/PKO BUILDING 1, AREA C WRIGHT-PATTERSON AFB, OH 45433-5320
	FAX NO. 513/257-3926

Security class (U,C,S,TS) : U ONR resident rep. is ACO (Y/N): N
Defense priority rating : DO S10 GOVT supplemental sheet
Equipment title vests with: Sponsor GIT

Administrative comments -
INITIATION OF FIRM FIXED PRICE PURCHASE ORDER.



GEORGIA INSTITUTE OF TECHNOLOGY
OFFICE OF CONTRACT ADMINISTRATION

NOTICE OF PROJECT CLOSEOUT

Closeout Notice Date 01/21/93

Project No. E-27-661_____

Center No. 10/24-6-R7489-0A0_

Project Director KUMAR S_____

School/Lab TEXT ENGR_____

Sponsor AIR FORCE/WRIGHT-PATTERSON AFB, OH_____

Contract/Grant No. F3360192MY642_____

Contract Entity GTRC

Prime Contract No. _____

Title UNDERSTANDING THE HIERARCHIAL STRUCTURE IN THE LIQUID CRYSTALLING POLYMER

Effective Completion Date 920815 (Performance) 920930 (Reports)

Closeout Actions Required:

	Y/N	Date Submitted
Final Invoice or Copy of Final Invoice	Y	_____
Final Report of Inventions and/or Subcontracts	N	_____
Government Property Inventory & Related Certificate	N	_____
Classified Material Certificate	N	_____
Release and Assignment	Y	_____
Other _____	N	_____

Comments EFFECTIVE DATE 5-9-92. CONTRACT VALUE \$12,000. _____

Subproject Under Main Project No. _____

Continues Project No. _____

Distribution Required:

Project Director	Y
Administrative Network Representative	Y
GTRI Accounting/Grants and Contracts	Y
Procurement/Supply Services	Y
Research Property Management	Y
Research Security Services	N
Reports Coordinator (OCA)	Y
GTRC	Y
Project File	Y
Other HARRY VANN-FMD _____	Y
FRED CAIN-ODD _____	Y

**TEMPERATURE DEPENDENT TORSIONAL MODULUS STUDIES OF
THERMOTROPIC LIQUID CRYSTALLINE POLYMERIC FIBERS**

by

**Students: Munish Shah & Vinay Mehta
Principal Investigator: Professor Satish Kumar
School of Textile & Fiber Engineering
Georgia Institute of Technology, Atlanta, GA**

**Technical Monitor: Professor A. N. Palazotto
Department of Aeronautics & Astronautics
Air Force Institute of Technology - NY
Wright Patterson Air Force Base OH 45433**

**Final Report for Contract #F3360192MY642
Project Title: Understanding The Hierarchical Structure in The Liquid
Crystalline Polymeric Fibers.**

September 23, 1992

Liquid Crystalline Polymer

The liquid crystalline behavior of polymers is a result of chain rigidity. A limited number of rod like chains can be accommodated in random arrangement in a solution, at higher polymer concentration local order between the chain molecules will exist. Schematic diagrams of isotropic and anisotropic phases are given in Figure 1. Polymers which show the liquid crystalline phase as a function of temperature are known as thermotropic liquid crystalline polymers. For a thermotropic LCP a turbid liquid phase may exist between the melting point of the crystalline phase and the isotropic, non-turbid liquid phase [1]. In contrast, some polymers exhibit mesomorphic behavior as a function of their concentration in solution; that is, if number of rod like polymer chains exceed certain critical concentration than a liquid crystalline phase forms; these are known as lyotropic liquid crystals. The characteristic features of lyotropic and thermotropic liquid crystalline polymers are shown in Figure 2(a) and 2(b). As shown in Figure 2(a), in the lyotropic liquid crystals, the solution viscosity initially increases with increase in polymer concentration, and then it decreases. The concentration at which the viscosity begins to decrease, represents the concentration at which the polymer goes into the anisotropic phase. The typical behavior of thermotropic liquid crystalline polymer is shown by the Differential Scanning Calorimetry scan in Figure 2(b). In this Figure, T_1 represents the glass temperature, T_2 is the melt temperature. The region between T_2 and T_3 represent the liquid crystalline (anisotropic) phase. Above T_3 , the system is in the isotropic amorphous melt state.

Based on chemical structure, liquid crystalline polymers (LCP) are categorized into two types (Fig 3): a main chain LCP which involves a succession of rigid molecular structures in the main chain to give a stiff chain with high axial ratio (ratio of length of a molecule to its diameter), and a side chain LCP which involves rigid molecular structures on the side of the main chain[2].

Furthermore, in a liquid crystal, polymer molecules can be arranged in three different ways (Fig 4).

1. Nematic LCP in which molecules show parallel one dimensional order (chain ends are not aligned).
2. Smectic LCP in which molecules align parallel and stratified with two

dimensional order in a coterminal manner.

3. Cholesteric LCP which consists nematic layers arranged in helical structure [3].

A hierarchical fibrillar structure model has been developed by L.C. Sawyer and M. Jaffe for highly oriented liquid-crystalline polymers in the forms of fibers and films. This model was first developed for thermotropic copolyester Vectra™ and then extended for the lyotropic LCPs, such as Kevlar™ and poly(p-phenylene benzobisthiazole). The fibrillar morphology was conformed after extensive characterization using broad range microscopy techniques such as Light microscopy, TEM, and SEM. Furthermore, recent studies using Field Emission Scanning Electron Microscopy (FESEM) and Scanning Tunneling Microscopy (STM) delineates a microfibrillar structure within the fibrillar structure [11]. According to Sawyer et al, microfibril does not arise due to fracture deformation but rather exists as a unit of fibrillar structure of LCPs. Microfibril are composed of two to five molecules and thus can be termed macromolecular in nature. Microfibril exhibits a tap-like shape. Also, kink band results due to deformation of the microfibril [11]. The LCP structural model consisting of elongated well-known fibrils give rise to high anisotropy .

Owing to the aromatic nature of the structure (Fig 5) both lyotropic and thermotropic liquid crystalline polymers generally possess combination of properties such as high heat distortion and service temperature, high chemical resistance, high tensile properties, flame retardancy without the need of additives; this enables LCP for Hi-Tech applications.

The theoretical development on the basis of the thermodynamics for the prediction of liquid crystalline behavior for a complete rigid chain was given in 1956 by P.J. Flory who used modified lattice theory and proposed a statistical theory of spontaneous ordering of rod like polymer molecules in concentrated solutions and melts. The theory specifically predicts that above a certain critical concentration, a rod like molecules that possess an axial ratio(x) greater than approximately 6.4 will spontaneously form two phases. At lower axial ratio, the phase is isotropic in which the molecules are completely uncorrelated; at higher axial ratio the phase is anisotropic in which the molecules are highly correlated with respect to their long axis resulting in appearance of a

stable anisotropic phase.

For processing thermotropic system requires a melting temperature at which polymer degradation and decomposition does not occur[2]. This is an necessary condition for processing of the TLCP melt. Chemical structural modifications are sought for achieving the reduction in melt temperatures for such systems. For example, phenyl groups can be linked by ethylene linkage for increased flexibility. With the introduction of more flexible group, the entropy change ΔS increases and hence melting temperature T_m decreases. The melt temperature of number of liquid crystalline polyesters is in the range of 280 to 350°C [4].

Thermotropic LCP possesses several processing advantages. For example, because the melt being ordered and having lower heat of fusion, very small amount of heat has to be removed when the mould is cooled and hence melt solidifies rapidly. This results in a short cycle time. Moreover, TLCPs possess low melt viscosity and hence long flow paths are achieved; therefore, the smallest mould can be filled [5]. The mechanical properties of thermotropic LCP are also influenced by processing parameters. Microfibrillar structures are formed within larger fibrillar structure during processing [11]. Fibrils forms a layered structure, with a long axis of the fibrils arranged along the extrusion direction due to shear and elongational flow arising during processing; this gives TLCP a wood-like, fibrous structure morphology. A range of exceptional properties, such as very good mechanical properties and low coefficient of linear thermal expansion results from this special morphology.

Because of exceptional properties and processing advantages of TLCPs several corporations are engaged in the development of TLCPs and are exploring the possibilities of application of TLCP fiber in composites and for electronic circuit, fiberoptics, and aerospace industry. A family of Vectra™ products are made by Hoechst Celanese[7].

VECTRATM:

Vectra™ is a high performance thermotropic Liquid Crystalline Polymer. The polymer is a thermotropic copolyester made from 4-hydroxybenzoic acid (HBA) and 2-hydroxy, 6-naphthoic acid (HNA)[6]. The chemical structure of the starting monomers and the repeat unit of Vectra™ are shown in Figure 6.

Hoechst Celanese further developed Vectran™ a multifilament spun fiber. The FESEM and STM studies reveals that Vectran™ has fibrillar morphology and the fibrils are not perfectly straight, neither they are perfectly align with the fiber or the tape axis but they wind in a serpentine fashion into and out of the longitudinal plane parallel to the fiber axis[11]. Figure 7 shows a schematic of the Vectran™ fiber structural model. The SEM studies of the fracture deformation of VectranHS due to tensile testing shows fibrillation (Fig 8).

The typical properties of Vectran™HS fiber are given in Table 1. The fiber exhibits exceptional mechanical and physical properties: High strength and modulus, high abrasion resistance, low moisture absorption, excellent chemical resistance, negative CTE, high impact resistance, high temperature resistance, excellent flammability resistance, and high dielectric strength [7].

EXPERIMENTAL:

A torsion pendulum is a simple method for measuring shear modulus and mechanical damping of a polymeric fiber. One end of the specimen is rigidly clamped and other is attached to a inertia disk, which is free to oscillate. The torsional pendulum arrangement is shown in Figure 9(a) and 9(b). The torsional modulus measurement were made on 6 sample of VectranHS fiber. 4 readings of each sample were taken. Measurements were made at 25°C, 60°C, 90°C,120°C, and 150°C. The samples were mounted on the cardboard tabs of one inch gage length. Epoxy glue was used for mounting the fibers on the tab, and the glue was allowed to set for 24 hrs. The radius of the sample was measured at 4 places along the one inch gage length by laser-beam diffraction method, using He-Ne laser. The radius of the fiber is given by the diffraction theory as

$$r = \mu S/\Delta$$

Where,

μ = wavelength of the laser (632.8 nm for the He-Ne laser)

S = distance between fiber and screen

Δ = distance of the first intensity minima from the main beam

The torsion pendulum was prepared using a cardboard disk. At the center of the disk a round head aluminum fastener was inserted for holding a bottom end of the paper tab containing the fibre sample. The top

end of the paper sample was clamped on the stand. Both side of the paper tab were cut carefully without straining the fiber so that the fiber can be freely attached to the torsion pendulum. The whole arrangement was placed in the vacuum oven, initially maintained at the room temperature. After mounting the specimen the vacuum was pulled. The fiber was set to rotate by letting very small amount of air in the oven chamber and the displacement period was recorded. The temperature of the oven was then raised to 60°C to measure displacement period for the rotation of the fiber at that temperature. Similarly measurements were taken at 90°C, 120°C, 150°C. The pendulum's moment of inertia was calculated by incorporating the contributions of cardboard disk, aluminum fastener and the lower portion of the paper tab. From the displacement-time data both the dynamic torsion modulus and logarithmic decrement Δ were calculated using the free-torsion pendulum equation[9]:

$$G = 8\pi^3 I L / A^2 T^2$$

Where,

I = moment of inertia of the pendulum = 0.2204 g-cm²

L = length of the fiber in cm

A = cross sectional area of the fiber in cm² = πr^2

T = corrected oscillation period given by

$$T = T_0 / (1 + (\Delta/2\pi)^2)^{0.5}$$

Where,

T_0 = measured period of the oscillation in seconds

Δ = logarithmic decrement = $\ln(A_0/A)$

A_0 and A are amplitude in two successive oscillations.

RESULTS & DISCUSSION:

From the Results (Table 2) it is clear that as the temperature increases torsional modulus of VectranHS decreases (Fig 10). This can be explained by considering chain and crystal structure, and orientation and the morphology of the fiber.

Vectran™ has fibrillar morphology; the crystals are closely packed. Under the torsion at high temperature the crystals may get distorted; as a result, torsional modulus may decrease. Also, crystal lattice distortion

may increase with increasing temperature; hence, there is greater amount of energy loss due to which damping increases (Fig 11). Moreover, since Vectra™ has negative CTE, the chains may shrink axially on heating and hence random coil morphology may initiate resulting into decrease in torsional modulus. Breakage of the dipole-dipole interaction on heating may further contribute to decrease in the torsional modulus.

Other studies carried out by us indicate that in the temperature range studied, the torsional modulus of all polymeric fibers decreases with increase in temperature, and the most significant decrease is observed in torsional modulus of Kevlar™ 49 and Vectra™. In the temperature range studied (room temperature to 150°C) no significant change in the torsional modulus of carbon fibers was observed. A comparison of the torsional moduli of the four polymeric fibers is given in Figure 12. Of these four high performance polymeric fibers Vectra™ has the lowest torsional modulus and kevlar™49 has the highest, with the intermediate values for PBZT and PBO. The low torsional modulus of Vectra™ is likely a result of -COO- group, as the rotation about -C-, and -O- will encounter little resistance. In Kevlar™ easy rotation around -NH- and -CO- is presumably resisted by the hydrogen bonding between adjacent chains, thus yielding higher torsional modulus for this fiber.

Damping factors is also capable of revealing some structural information about the fibers. However, in the case of fine fibers it must be ensured that the damping factor represents the true value for the fiber and that it is not a result of aerodynamic effects. Towards this end, it was concluded in a study by Adams & Lloyd[12] that for obtaining true fiber damping it was necessary to use very high vacuum levels (10^{-6} torr). Adams & Lloyd further contend that at higher than 0.1 torr the damping is essentially due to aerodynamic effects, and that at these vacuum levels fiber damping makes negligible contribution. However our study seems to indicate that the damping factors reported are the true damping factors.

References

1. Russell A. Gaudiana, Polyesters, mainchain Aromatic, in The Encyclopedia of Polymer Science and Engineering, John Wiley and Sons, New York, Index Volume, p.264, (1990).
2. S.L. Kwolek, P.W. Morgan, J.R. Schaefgen, Liquid Crystalline Polymers, in The Encyclopedia of Polymer Science and Engineering, John Wiley and Sons, New York, p.547, (1990).
3. Michael Jaffe, Gordon Caludann, Hyun-Nam Yoon, Fibers from Naphthalene-based thermotropic liquid crystalline copolyester, in High Technology Fibers, Part B (M. Lewin and J. Preston, Eds.), Marcel Dekker, New York, 1985.
4. Maged A. Osman, *Polymer* , v28 n5, p. 713-715,(1987).
5. G. Kirsch, H. Terwyen, *Kunststoffe-German Plastics* , v80 n10, p. 57-60, (1990).
6. Geoffrey R. Davies, Ian M. Ward, Structure and properties of oriented thermotropic liquid crystalline polymers in the solid state, in High Modulus Polymers (A.E. Zachariades, R.S. Porter, Eds.), Marcel Dekker, New York, 1988.
7. D.E. Beers, J.E. Ramirez, *Journal of the Textile Institute* , v81 n4, p.561-574, (1990).
8. T. Murayama, Dynamic Mechanical Analysis of Polymeric Material, Elsevier, Amsterdam, p.43-44,1978.
9. Satish Kumar, Vinay R. Mehta, David P. Anderson, Allan S. Crasto, Proc. 37th International SAMPE Symposium, March 1992, p. 967-973.
10. Charles E. McChesney, Liquid Crystalline Polymers, in the

Engineered Materials Handbook, ASM International, v2,
p.179-182, (1988).

11. L.C. Sawyer, R.T. Chen, M.G. Jamieson, I.H. Musselman, P.E. Russell, *Journal of Material Science Letters* , v11 n2, p.69-72, (1992).
12. R. D. Adams & D.H. Llioyd, *J. Phys. E. Scientific Instruments*, 8 (1975) 475.

Typical Properties of VectranHS

Tensile Strength	412 ksi (2.8 GPa)
Tensile Modulus	9.4 Msi (65 GPa)
Elongation at Break	3.3 %
Melting Point	625° F (330° C)
Moisture Regain	<0.1 %
Dielectric Constant @1 KHz	3.3
Density	1.4 g/cc (0.05 lbs/in ³)
Chemical Resistance	Hydrolytically stable
Resistance to organic solvents	

Table 1. Mechanical and physical properties of VectranHS.

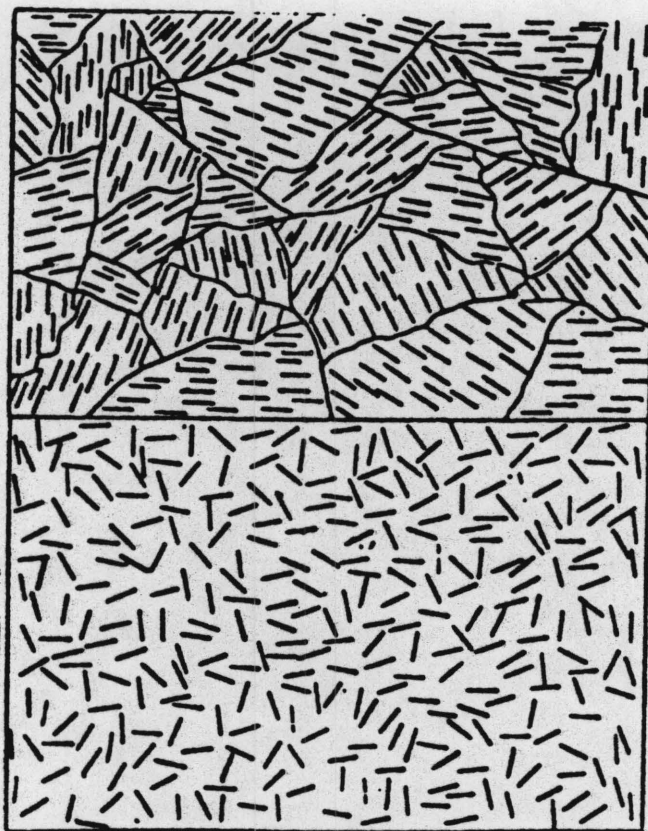
Temperature (°C)		G (GPa)	Std. Deviation	Δ	Std. Deviation
1.	26	0.59	0.035	0.594	0.050
2.	60	0.39	0.030	0.785	0.113
3.	90	0.25	0.046	1.170	0.250
4.	120	0.20	0.050	1.170	0.390
5.	150	0.18	0.040	1.380	0.450

Table 2. Experimental results of the temperature dependence study of torsional modulus and damping factor of VectranHS.

Fiber	Tensile Strength (GPa)	Tensile Modulus (GPa)	Density (g/cc)	Torsional Modulus (GPa)	Compressive Strength (GPa)
Kevlar™ 49	3.5	125	1.44	1.9	0.39-0.48
Kevlar™ 149	3.4	185	1.47	1.2	0.32-0.46
Spectra™ 1000	3.0	170	0.97	-	0.17
PBO	3.5-5.7	280-360	1.58	0.97	0.20-0.40
Vectran™HS	2.9	65	1.41	0.54	-
Pitch based Carbon fibers					
P-100	2.2	725	2.15	4.7	0.48
P-25	1.4	160	1.90	-	1.15
PAN based Carbon fibers					
T-300	3.2	235	1.76	15	2.88
T-50	2.4	390	1.81	14	1.61
Inorganic fibers					
S-Glass	4.5	90	2.46	-	>1.1
Al ₂ O ₃	1.7	350-380	3.7	-	6.90
SiC	3.45	400	3.0	-	-

Table 3. Mechanical properties of High Performance Fibers.

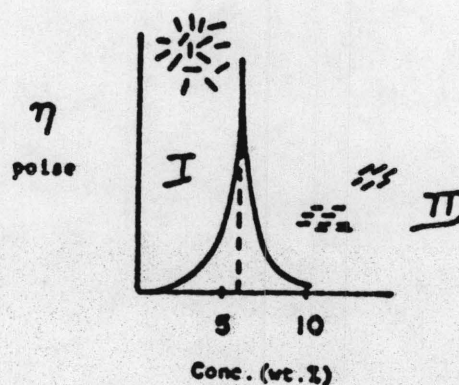
ANISOTROPIC PHASE



ISOTROPIC PHASE

Fig 1. Schematic diagrams of the anisotropic and isotropic phases in liquid crystalline polymers.

LYOTROPIC

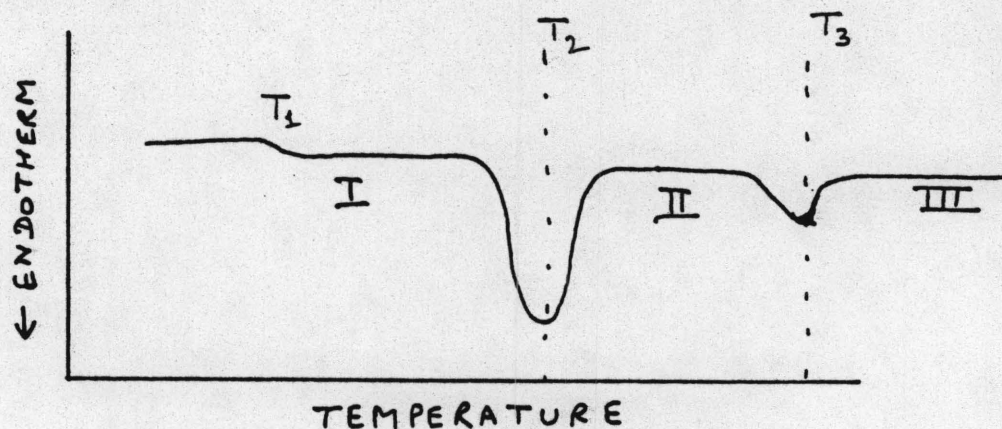


VISCOSITY AS A FUNCTION OF POLYMER CONCENTRATION IN SOLUTION

PHASE I: ISOTROPIC

PHASE II: ANISOTROPIC

THERMOTROPIC

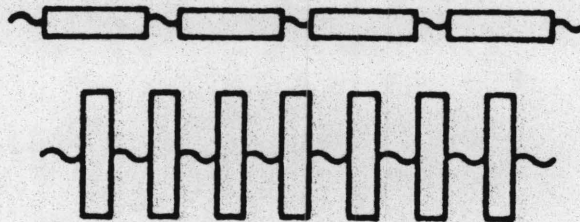


DIFFERENTIAL SCANNING CALORIMETRY PLOT AS A FUNCTION OF TEMPERATURE

REGION I: SEMICRYSTALLINE
REGION II: LIQUID CRYSTALLINE
REGION III: LIQUID LIKE

Fig 2 (a). Viscosity as a function of polymer concentration in a solution indicating lyotropic behavior and (b) the DSC plot as a function of temperature indicating thermotropic behavior of the LCP.

MAIN CHAIN LIQUID CRYSTALLINE POLYMERS



SIDE CHAIN LIQUID CRYSTALLINE POLYMERS

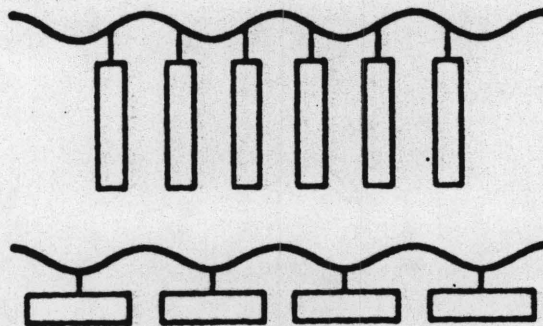


Fig 3. Classification of the LCP based on chemical structure.



Nematic

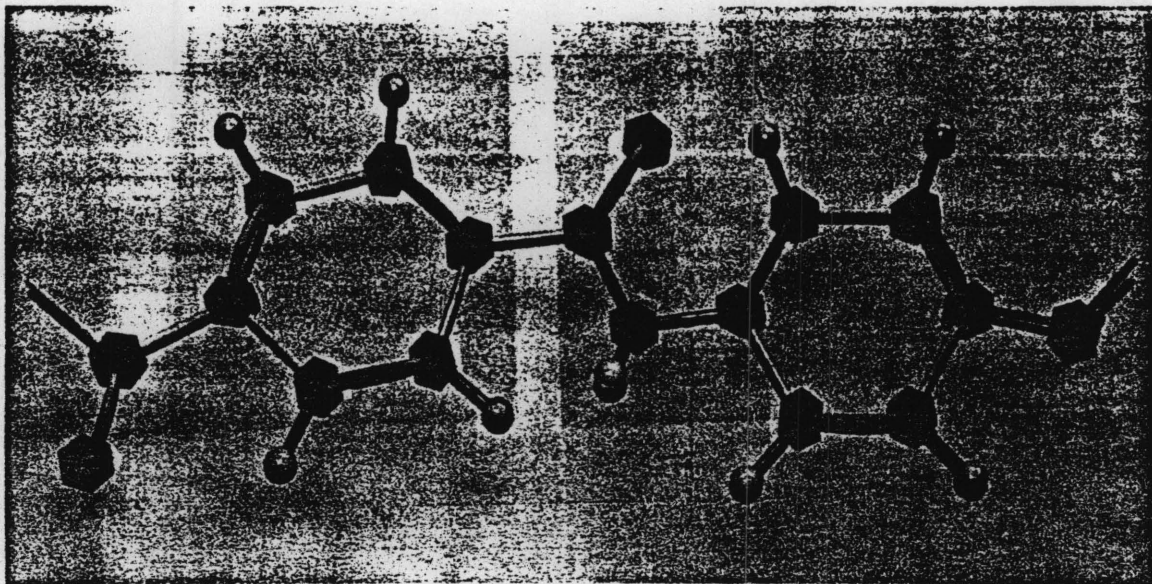


Smectic

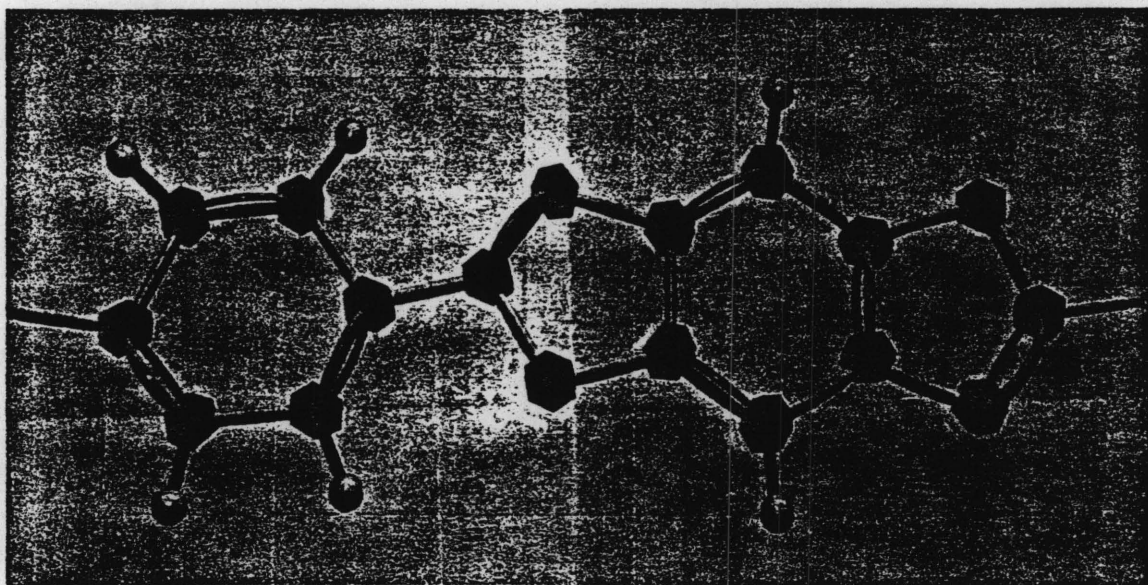


Cholesteric

Fig 4. Physical arrangement of the molecules in the LCP.

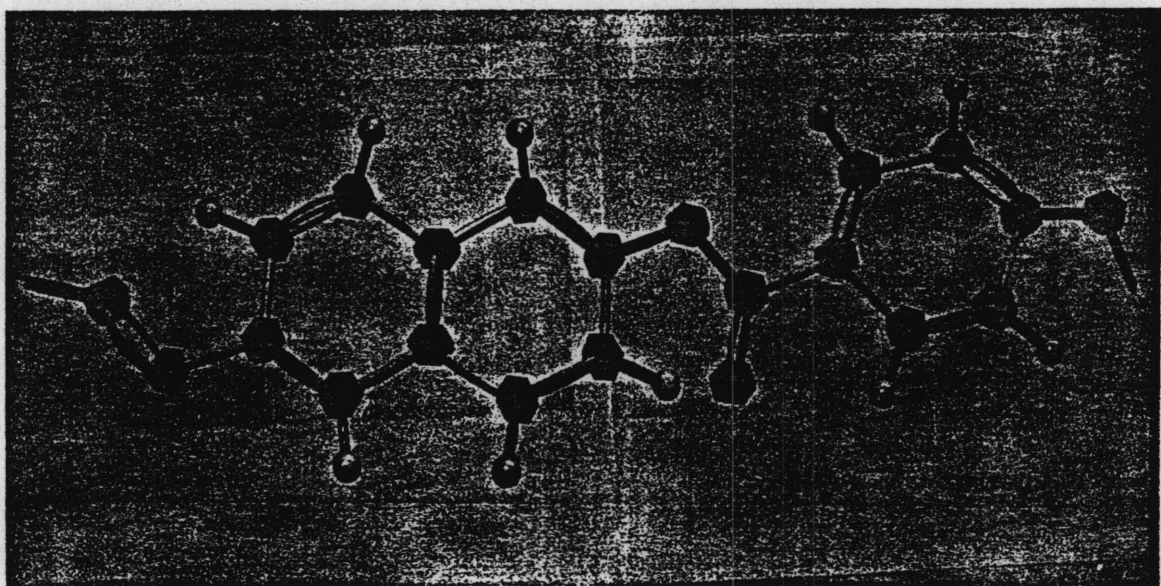


Kevlar™



PBZT

Fig. 5. Chemical Structures of LCPs.



Vectra™

(cont.)
Fig 5_A Photographs of the chemical structural model of the LCPs.

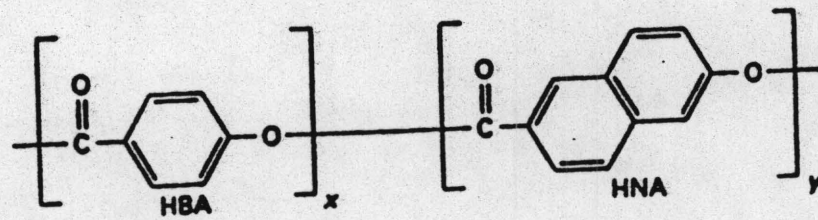
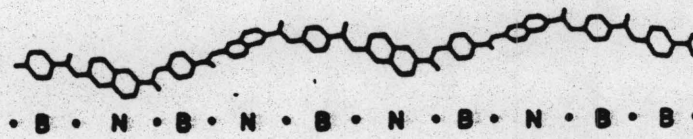
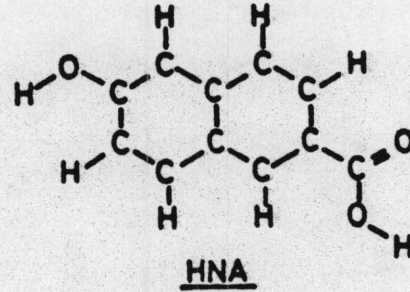
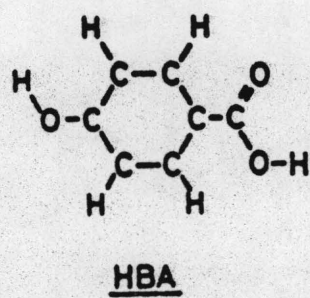


Fig 6. Monomers of HBA and HNA which polymerize to give thermotropic copolyester Vectra™.

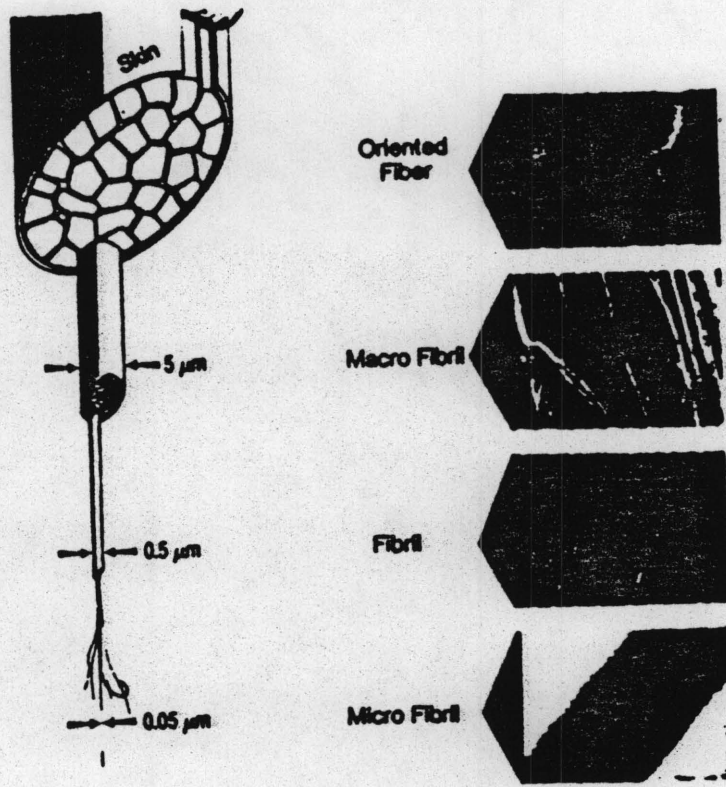


Fig 7. Morphology model of VectranTM.

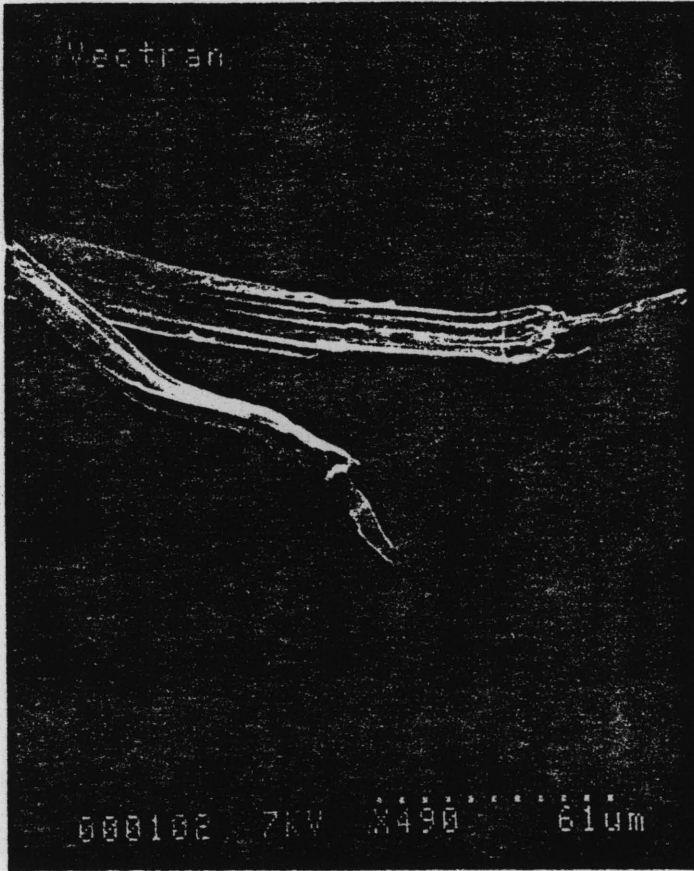


Fig 8. Micrographs of the fracture deformation due to tensile test of VectranHS showing fibrillation.

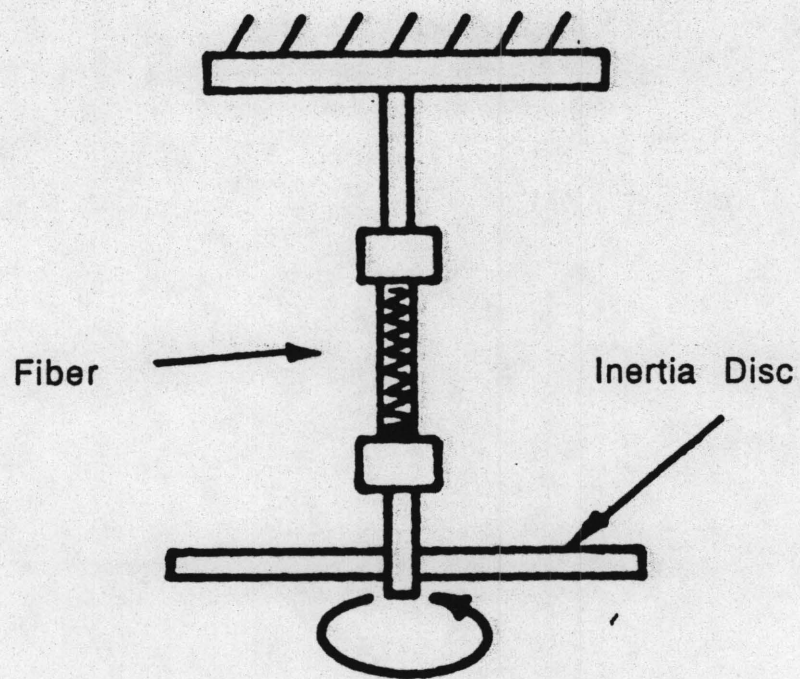


Fig 9(a). Schematic diagram of a torsional pendulum.



Fig. 9(b). Experimental set-up of the torsional modulus apparatus.



Fig 9(b). Photographs of an experimental set-up to study torsional modulus of a fiber.

Plot of Torsional Modulus Vs. Temperature of Vectra

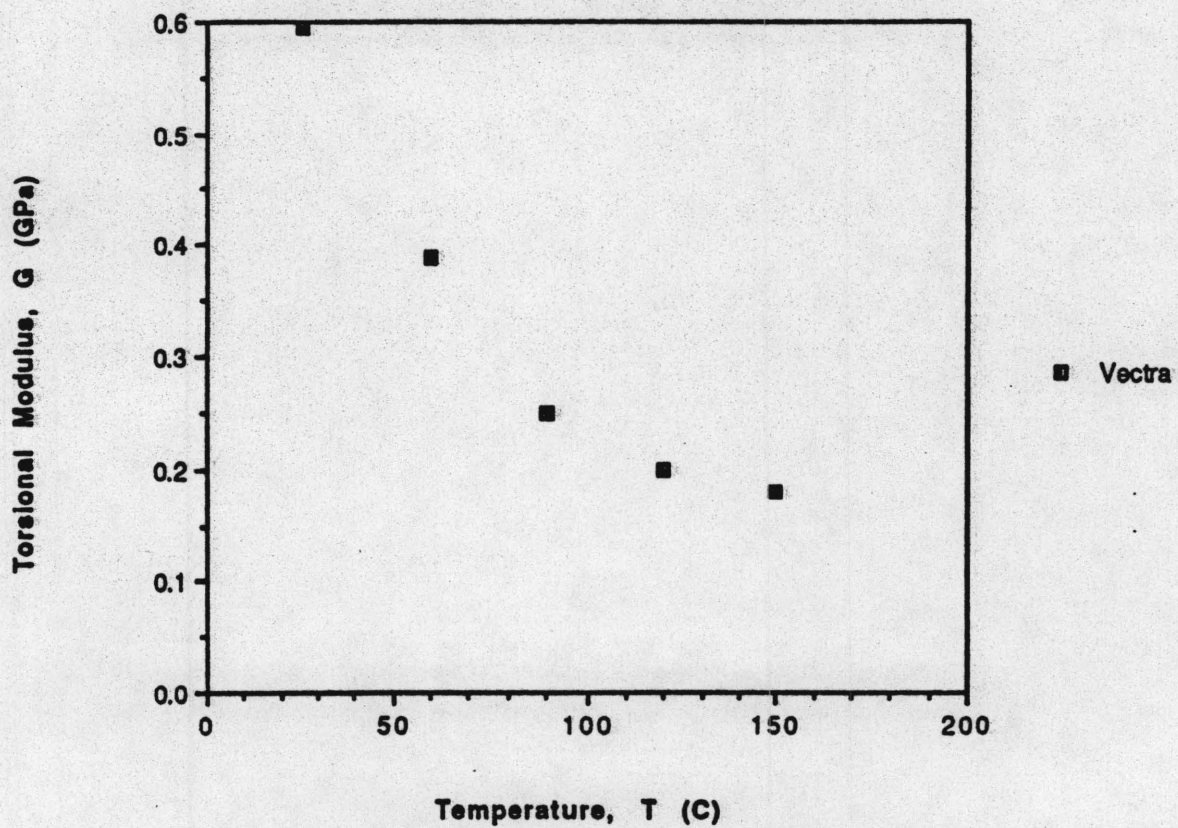


Fig 10. Behavior of torsional modulus of VectranHS with temperature.

Plot of Damping Factor Vs. Temperature

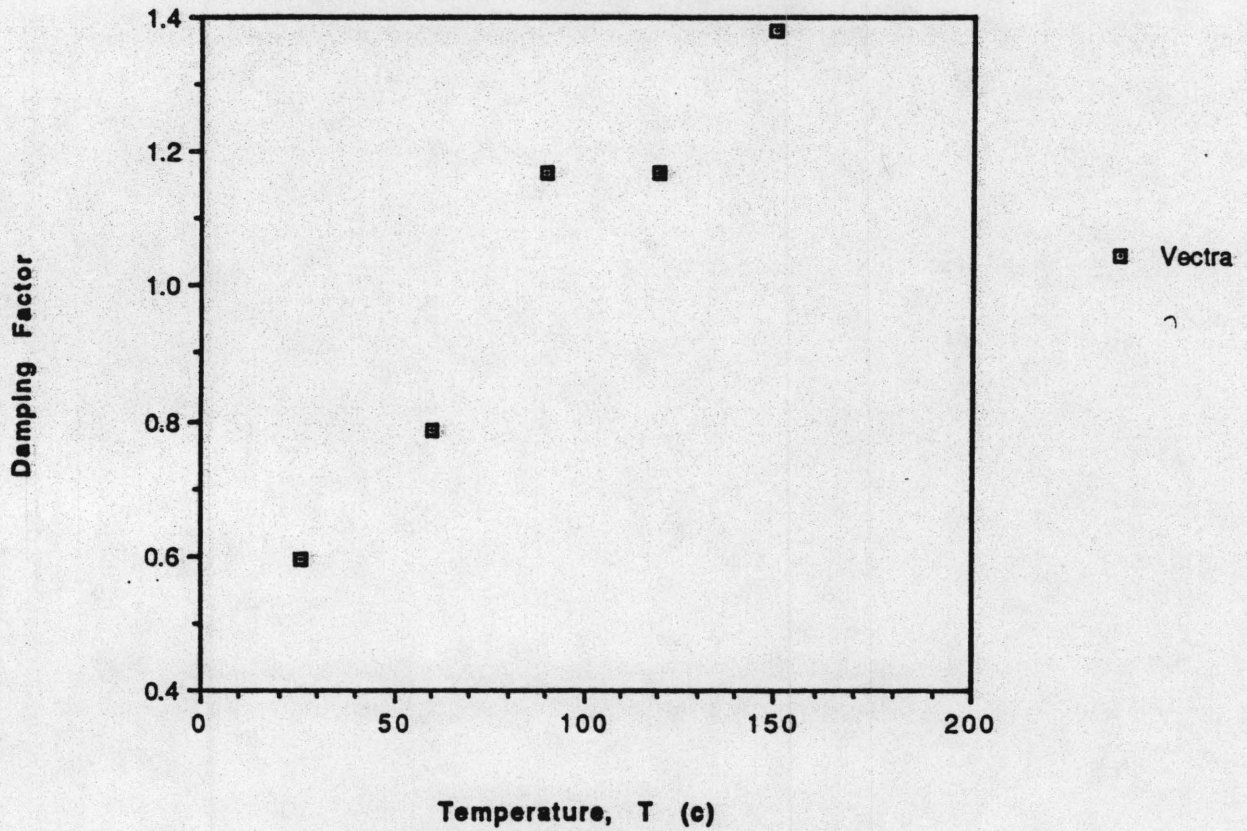


Fig 11. Behavior of damping factor with temperature for the torsional modulus studies of the VectranHS.

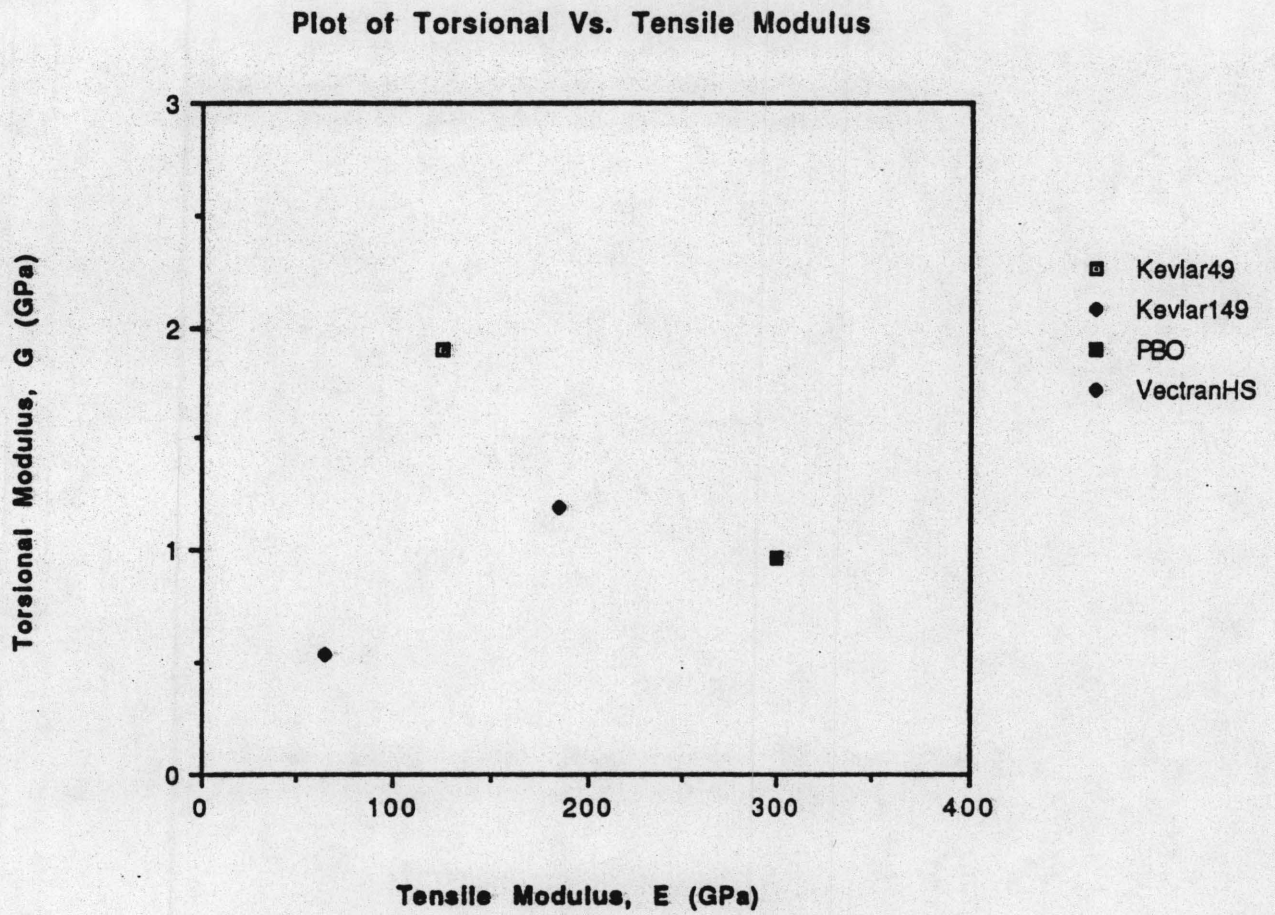


Fig 12. Plot of torsional modulus Vs. tensile modulus of various LCP fibers.